REPORT OF HYDROGRAPHIC RESEARCHES No. 14, March, 1979

STATISTICS ON THE CURRENTS IN THE SEAS ADJACENT TO JAPAN

Hideo Nitani*, Shozo Yoshida*, Jun Okumoto* and Hiromi Nakamura*

Received 1978 September 18

Abstract

Statistics on the currents in the seas adjacent to Japan have been carried out with use of approx. eighty thousand GEK data observed from 1953 to 1970. The statistics have been conducted for the vector mean, scalar mean, maximum velocity, stability and standard deviation in three statistical periods, the periods in which the large meander of the Kuroshio off Kishu and Enshu-nada is both absent and present, the overall period from 1953 to 1970. Although the detailed characteristics can be seen from the statistical atlases attached, the comprehensive characters of each statistical element in each region, and the relationships among them, are described. In general, the distributional pattern of each element is similar to each other, especially in the region of the Kuroshio. The variability, defined as (standard deviation)/(stability), of the Kuroshio propagates from west to east, and is larger in the period when the large meander is absent than in the period of its presence. A characteristic linear relationship between vector mean and scalar mean is significant in each region, and the other relationships between each element, except the maximum velocity, can be introduced from this basic relationship.

1. Introduction

In 1935 and 1936 the atlases of the ocean currents in the Northwest Pacific and the North Pacific were published by Hydrographic Office of Japanese Navy. After the World War II, US Naval Oceanographic Office issued three kinds of current atlases for the Northwest Pacific and its adjacent seas. In these atlases, the currents were shown mainly by the vector mean in each one degree mesh of longitude and latitude based on the statistics of the ship drift data of the naval merchant, and research vessels.

In recent years, Rikiishi (1974) and Rikiishi and Umatani (1977) computed the mean vector of the current and its stability in the Kuroshio region by the use of GEK data provided by the Japan Oceanographic Data Center (JODC). They described some characteristic features of the Kuroshio, from the statistical view point, in the both periods in which the large meander of the Kuroshio off Kishu and Enshu-nada is absent and present.

In 1971, JODC initiated the collection of the GEK data, which had been accumulated from 1953 in Japan, and carried out some statistics on the current velocity to investigate the relation between the surface transport (integration of the surface current with distance) and abnormal high sea level along the southern coast of Japan occured in September of that year (Nitani, 1974). Later, additional statistics have been carried out by JODC with use of about eighty thousand GEK data to compile a new atlas *Marine*

* Japan Oceanographic Data Center

Environmental Atlas III which will be issued in early 1979 adding more data obtained in the period 1971–1977. As the results of these statistics, several characteristics of the distribution of the statistical elements such as vector mean, scalar mean, maximum velocity, stability and newly defined standard deviation of the current and the relationships among them are discussed in the present paper.

2. Method of the Statistics

(1) Data source

Data used in this statistics are those observed almost by the Japanese research agencies in the period from 1953 to 1970 (Table 1). The number of the data in each 30′ mesh is shown in Plate 1. The isopleths run, in general, parallel with the Japan Islands but those nearly perpendicular to the coast, along the regular observational lines of each agency, are remarkable in the Japan Sea and the eastern offing of Tohoku district. This means paradoxically that the observations in the Kuroshio region are conducted with the comparatively uniform basis and further that the regular observational lines are dense in space.

Table 1 Number of GEK data used in the statistics

Observed Year	Number of Data						Total
	MSA	JMA	FA, PFE	DA	Univ.	USSR	
1953	86						86
1954	1,001						1,001
1955	1,907	198					2,105
1956	2,957	933					3,890
1957	2,739	1,564			43		4,346
1958	3,566	1,546			78		5,190
1959	2,971	1,437					4,408
1960	3,654	1,497					5,151
1961	3,318	1,712			46		5,076
1962	2,934	1,478			39		4,451
1963	2,916	1,820					4,736
1964	3,038	1,949	820				5,807
1965	3,431	1,961	590		31		6,013
1966	3,692	1,893	611		89		6,285
1967	3,253	1,976	755		178		6,162
1968	3,454	1,191	707		140	123	5,615
1969	3,295	1,559	658		15	20	5,547
1970	3,094	1,803	725	106	58		5,786
Total	51,306	24,517	4,866	106	717	143	81,655

MSA : Maritime Safety Agency
JMA : Japan Meteorological Agency
FA : Fisheries Agency
PFE : Prefectural Fisheries Experimental Station
DA : Defense Agency

(2) Periods for the statistics

The statistics have been carried out with the use of all data simply to get the averaged state of each statistical element, and the same statistics for each season have been also conducted, where each season is defined as follows; the winter covers January–March the spring April–June, the summer July–September and the autumn October–November.

In addition to above, for the statistics in the Kuroshio region, the period has been divided into two periods according to the presence or absence of the well known large meander of the Kuroshio off Kishu and Enshu-nada. We shall call

Period A : all the period (whole period) 1953–1970 (B + C)
Period B : large meander absent (A − C)
Period C : large meander present Oct. 1953–Dec. 1955, Jul. 1959–Dec. 1962

The characteristics of the Kuroshio not only off Kishu and Enshu-nada but also off other districts vary according to the presence of this large meander.

(3) Geographical unit for the statistics

The statistics have been carried out for every 15′, 30′ and 1° meshes in longitude and latitude, but only the results of the statistics for every 30′ meshes are discussed in this paper.

(4) Statistical elements

The vector mean, scalar mean, maximum velocity, stability (vector mean/scalar mean) and standard deviation have been computed as the statistical element. The standard deviation is defined newly as $\sigma=(\sigma_E^2+\sigma_N^2)^{1/2}$, where σ_E and σ_N are the standard deviations of the east and north components of the velocity, respectively.

The relative frequency distributions of the current speed in the selected eighteen meshes have been also computed.

3. Results of the Statistics for All the Period

(1) Vector mean, $\bar{V}$ (Plate 2)

In the current axial areas, we find, as a rule, the considerably lower velocities than those in the actual current because of the averaging process in time and space.

The most parts of the region south of Japan are occupied by the Kuroshio and its countercurrent south of it. The regions where vector mean is larger than 0.5 knots and 1.0 knot correspond to the Kuroshio region in wide sense and its axial area, respectively. The mean velocities of the axial area of the Kuroshio southeast of Kyushu and near Izu Ridge decrease to the values less than 1.0 knot suggesting the intense variation of path of the Kuroshio in these regions, as seen from the pattern of stability shown later. Off Kii Peninsula, a tongue-like high velocity area, in which the current flows southeast, extends to south owing to the effect of the presence of the large meander of the Kuroshio there. We can find the several isolated isopleths of 0.2 knots along the boundary zone between the Kuroshio and its countercurrent south of it. Especially, the warm core south of Shikoku is remarkable.

In the eastern offing of the northern Tohoku district, the Tsugaru Warm Current and its extention along the coast are remarkable as well as so called the second branch of the Oyashio along the longitudes of 145°–146°E.

In the Japan Sea, the vector mean in the coastal and offshore branches of the Tsushima Warm Current is only 0.2–0.4 knots, and the area in which the vector mean is less than 0.2 knots occupies the comarative wide region in the both sides of the offshore branches. The low vector mean is due to not only low velocity of this current

but also to the large variability of the current in time and space. The dispersed current branches converge in the southwestern region of Tsugaru Strait and reach about 0.5 knots in vector mean. Because of the weakness of the velocity and small number of the data in the regions of the East Korean Warm Current and in the Liman Current, we can not find definite structures.

(2) **Scalar mean,** $\overline{V}$ (Plate 3)

The pattern of the distribution of the scalar mean of the current is fairly similar to that of vector mean in general, though the detailed relationship between two elements may have the characteristic in each current region.

As a rule, the value of $\overline{V}$ in each mesh is larger than that of $\overline{\boldsymbol{V}}$ and their ratio $\overline{\boldsymbol{V}}/\overline{V}$ increases with $\overline{\boldsymbol{V}}$ or $\overline{V}$. The maximum value of $\overline{V}$ reaches to 2 knots in the axial area of the Kuroshio southeast of Kii Peninsula.

(3) **Maximum velocity,** $\boldsymbol{V}_{\max}$ (Plate 4)

At first, we must be careful in the interpretation of Plate 4 showing the distribution of $\boldsymbol{V}_{\max}$, because the larger $\boldsymbol{V}_{\max}$ appears with increasing number of the data in each mesh as expected from the extreme problem and hence, the values in Plate 4 may not mean the actual maximum values.

We find the high $\boldsymbol{V}_{\max}$ lager than 4 knots in Kuroshio axial area (including the Kuroshio extension) east of Shikoku as well as in the Tsugaru Strait. The highest $\boldsymbol{V}_{\max}$ arroud Japan may be in the order of 5.5 knots or so.

$\boldsymbol{V}_{\max}$ exceeds 3 knots everywhere in the Kuroshio region in wide sense, but there is no $\boldsymbol{V}_{\max}$ higher than 3 knots in the Japan Sea except in the Tsugaru and Soya Straits. In general, $\boldsymbol{V}_{\max}$ in the southeastern half of the Japan Sea exceeds 1.5 knots but that in northwestern half does not exceed 1 knot mostly.

(4) **Stability,** $S\,(=\overline{\boldsymbol{V}}/\overline{V})$ (Plate 5)

This quantity may be considered as a measure of the variability of the current direction. The pattern of its distribution is similar to those of $\overline{\boldsymbol{V}}$ and $\overline{V}$, especially in the strong current regions.

The larger values more than 0.8 (80%) are found in the Kuroshio axial area and even the values more than 0.9 off Shikoku, Kii Peninsula, Enshu-nada and in the East China Sea. The small values less than 0.4, sometimes less than 0.2, are found at the coastal region and boundary zone between the Kuroshio and its countercurrent south of it. The values in the Oyashio region and the Japan Sea are small in general. In the Tsugaru and Soya Straits, however, they exceed 0.8.

(5) **Standard deviation,** σ (Plate 6)

We can introduce another measure for the variabilty of the current other than the stability mentioned above. The standard deviation of the current is defined as the vector resultant of the standard deviations of east and north components, σ_E and σ_N, of the velocity. Horizontal and vertical lengths of plus (+) marks in Plate 6 indicate the magnitude of σ_E and σ_N respectively, and the figure below plus mark is the resultant value, $\sigma\,(=\sqrt{{\sigma_E}^2+{\sigma_N}^2})$.

Also σ may be defined as the standard deviation of the scalar quantitiy ΔV_i of

the vector anomalies ΔV_i from the top of the mean vector $\overline{V}$ to the tops of the individual vectors. In the practical computation, we use the root of the invariable variance as the standard deviation.

In general, the distributional pattern of σ is also comparatively similar to each element already described. The large values more than 1 knot are found in the Kuroshio region and the Tsugaru and Soya Straits, and the largest values more than 1.5 knots are found only in the Kuroshio axial areas off Enshu-nada and in the Kuroshio extention.

In the Kuroshio region off Shikoku and in the East China Sea, the values are not so large owing to the large stability in these regions. This may be expected from the simple consideration that large standard deviation will associate with the small stability and large velocity or speed of the current.

4. Characteristic Features of Each Statistical Element in the Periods B and C

In the period B, the large meander of the Kuroshio was absent, but small- and medium-scale meanders propagated from west to east with the phase velocity of about 5 nauti. mile/day two or three times a year (Nitani 1975). On the contrary in the Period C, the large meander of the Kuroshio located off Kishu and Enshu-nada for several years almost stationarily associating with the large cold water mass inside of it. In the both periods, the distributions of the statistical elements of the current as well as other elements such as temperatute and salinity differ from each other.

As a rule, in the regions to which influence of the existance of the large meander may reach, the values of $\overline{V}$, $\overline{V}$ and $\overline{V}/\overline{V}$ in the Periods B and C are larger than those in all the period (Period A), and σ is contrary owing to the comparative uniformity of the current in each divided period.

As shown in Plate 7, the ratio of the number of the data used in the Period B to that in the Period C is about 3 : 1, in proportion to the duration of the respective periods. Accordingly, the pattern of each statistical element in all the period (Period A) is more similar to those in the Period B than in the Period C.

The detailed characteristic features of both periods (B and C) in the Kuroshio region will be seen by Plates 8–12, but some remarkable or common features are described below.

At first we can see that the elements in each period are comparatively similar to each other within that period as same as the case for the Period A. Accordingly the patterns of all elements are classified into two patterns depending on the paths of the Kuroshio in the both periods. The paths of the Kuroshio off Shikoku and Enshu-nada in the Period C locate farther from the coast than those in the Period B and the contrary is seen in the Kuroshio region east of Izu Ridge.

The area of high vector mean in the Period C, e.g. more than 1 knot, continues as a belt from the region southeast of Kyushu to offing of Tohoku district, but in the Period B such a belt is broken down near Izu Ridge and diverges in the region east of Izu Ridge. This phenomenon may be due to the tendency that the small- and medium-

scale meanders proceeding east grow rapidly in the offing of Enshu-nada being affected by the shallow topography of Izu Ridge in certain manner. The complicated topography of Izu Ridge also may contribute to the divergence of the flow at the Izu Ridge and east of it.

As indicated by Rikiishi (1977), the path and the mean velocity in the Kuroshio extension are more stable and larger in the Period C than in the Period B. The same tendency is slightly seen in the Kuroshio region southeast of Kyushu and south of Shikoku.

As a rule, the stability in the Period C is larger than those in the Period B and the differences in $\overline{V}$, $\overline{V}$ and the wideness of the strong current area in both periods are not so remarkable so far as we compare from the statistics, although the strongest part of the axial area is found almost to the east and the west of Kii Peninsula corresponding to the Periods B and C, respectively. It is also difficult, from these statistics, to say that in which period the average of the actual velocity of the Kuroshio axial area at the individual times is stronger.

For the maximum velocity, the values in the Period B are larger by about 1 knot than those in the Period C. But considering the difference of the number of the data used in the both periods we can not say also that in which period the true V_{max} is larger.

5. Relationships among the Statistical Elements

The relationships among $\overline{V}$, $\overline{V}$, $\overline{V}/\overline{V}$, V_{max} and σ and their characteristics in six

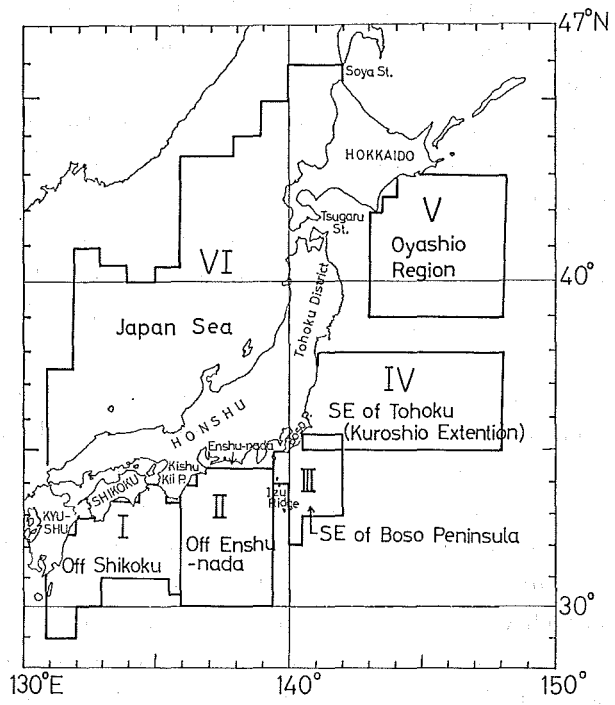

Figure 1 Subdivision of the region into six representative regions

representative regions shown in Figure 1 are discussed. Four of six regions are in the Kuroshio region and other two are in the Oyashio region and the Japan Sea.

(1) $\overline{V}\sim\overline{V}$

The relationship between $\overline{V}$ and $\overline{V}$ in each region can be expressed by the equation,

$$\overline{V}=a\overline{V}+b\ , \qquad (1)$$

especially for Regions I-IV as shown in Figure 2 in which the statistical values in every meshes and the regression lines for all the period (Period A) are indicated together with the regression lines for the Periods B and C. The coefficients a and the constant b in (1) obtained by the method of least squares and the correlation coefficient between $\overline{V}$ and $\overline{V}$ in each region are shown in Table 2.

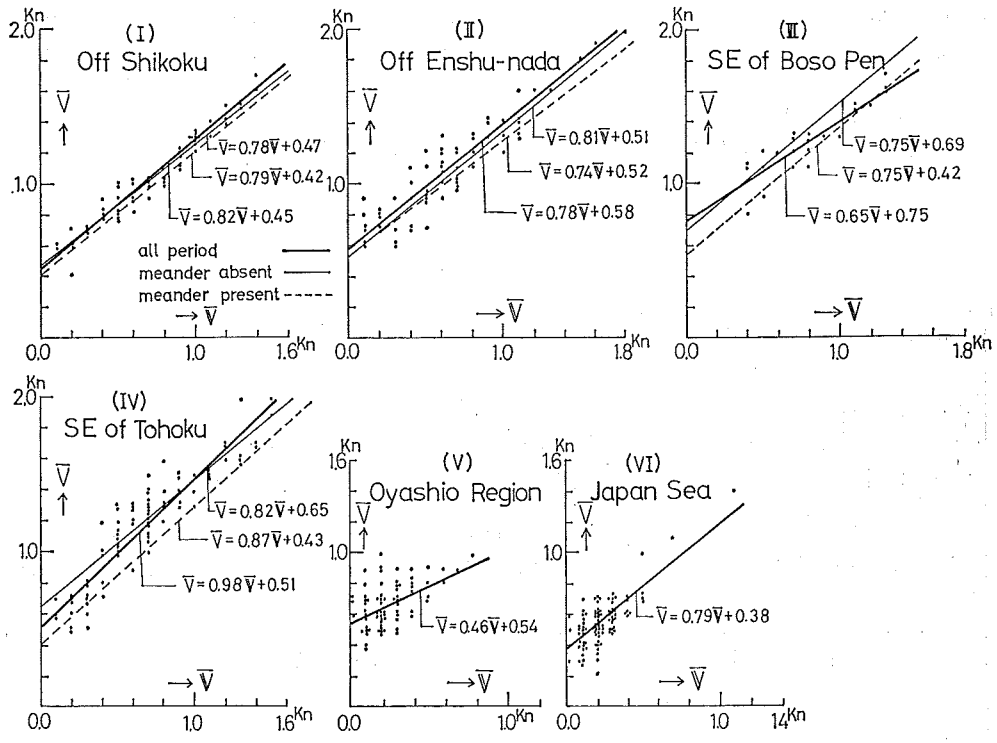

Figure 2 Relationship between $\overline{V}$ and $\overline{V}$ with the statistical values in the Period A and the regression lines for the Periods A, B and C

The correlation coefficients in the Regions I-III and the Region IV are larger than 0.9 and 0.8 respectively, and those in the Oyashio region and the Japan Sea (Regions V and VI), where the currents are not so strong, are small.

The values of a in the all regions are less than unity meaning that the increase of $\overline{V}$ in each region is larger than that of corresponding $\overline{V}$ owing to the increase of the convergence of the direction of the current with increasing velocity.

The values of b in Table 2 suggest that even if the definite current is absent in the seas adjacent to Japan, there exists the current of about 0.5 knots on the average

having no definite direction.

Table 2 Relation between $\overline{\boldsymbol{V}}$ and $\overline{V}$

Region	Period	Correla. Coeff.	a	b
I (Off Shikoku)	A	0.97	0.82	0.45
	B	0.97	0.78	0.47
	C	0.96	0.79	0.42
II (Off Enshu-nada)	A	0.93	0.78	0.58
	B	0.94	0.81	0.51
	C	0.91	0.74	0.52
III (SE of Boso Penin.)	A	0.90	0.65	0.75
	B	0.92	0.75	0.69
	C	0.95	0.75	0.53
IV (Kuroshio Ext.)	A	0.87	0.98	0.51
	B	0.83	0.82	0.65
	C	0.92	0.87	0.43
V (Oyashio Region)	A	0.44	0.46	0.54
VI (Japan Sea)	A	0.71	0.79	0.38

(2) $S\sim\overline{\boldsymbol{V}}$ or $\overline{V}$

From (1) the relation between S and $\overline{\boldsymbol{V}}$ or $\overline{V}$ is given by

$$S=\frac{1}{a+\dfrac{b}{\overline{\boldsymbol{V}}}} \qquad (2)$$

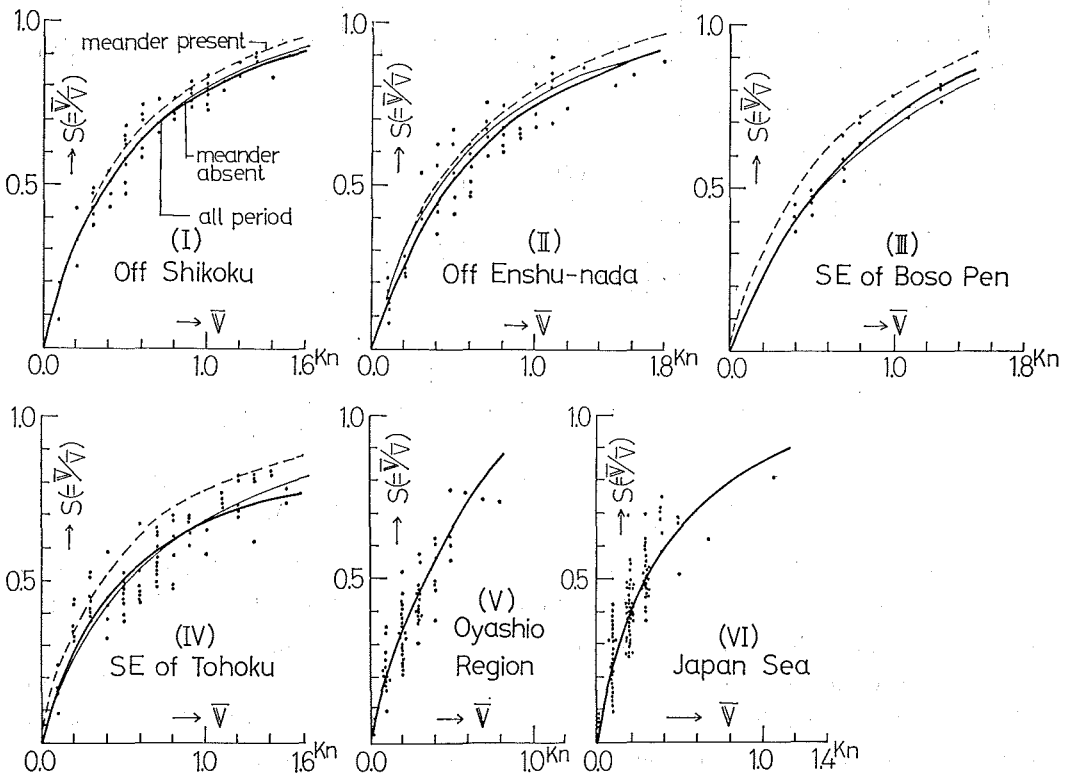

Figure 3 Relationship between $S\,(=\overline{\boldsymbol{V}}/\overline{V})$ and $\overline{\boldsymbol{V}}$ with the statistical values in the Period A and the calculated lines for the Periods A, B and C

or

$$S=\frac{1-\frac{b}{\overline{V}}}{a} \qquad (3)$$

where a and b are characteristic values in each region.

From this relation, Stability S increases with increasing $\overline{V}$ or $\overline{V}$ and decreases with increasing a and b. The computed values by (2) accord with the statistical values fairly well (Figure 3). In the Kuroshio axial area, especially in the Regions I and II, we can find large S owing to the high velocity. Also, in the Kuroshio region S is larger in the Period C than in the Period B due to the comparatively small a and b in the Period C as shown in Table 2.

In the Oyashio region, the stability is less than 0.5, in general, in spite of very small a, because $\overline{V}$ is less than 0.5 knots except in several meshes. In the Japan Sea, S is also small except in and west of the Tsugaru Strait, because $\overline{V}$ is small and a and b are not so small in this region.

(3) $\sigma\sim\overline{V}$, $\overline{V}$ and S

From the definition of the standard deviation σ, it is expressed by

$$\begin{aligned}\sigma^2&=\sigma_E{}^2+\sigma_N{}^2=\frac{1}{n}\sum_{i=1}^{n}\{(V_{iE}-\overline{V}_E)^2+(V_{iN}-\overline{V}_N)^2\}\\&=\frac{1}{n}\sum_{i=1}^{n}(V_{iE}{}^2+V_{iN}{}^2)-(\overline{V}_E{}^2+\overline{V}_N{}^2)\\&=\frac{1}{n}\sum_{i=1}^{n}V_i{}^2-\overline{V}^2\ ,\end{aligned} \qquad (4)$$

where n is the number of the data in each mesh.

If we put $V_i=\overline{V}+\Delta v_i$,

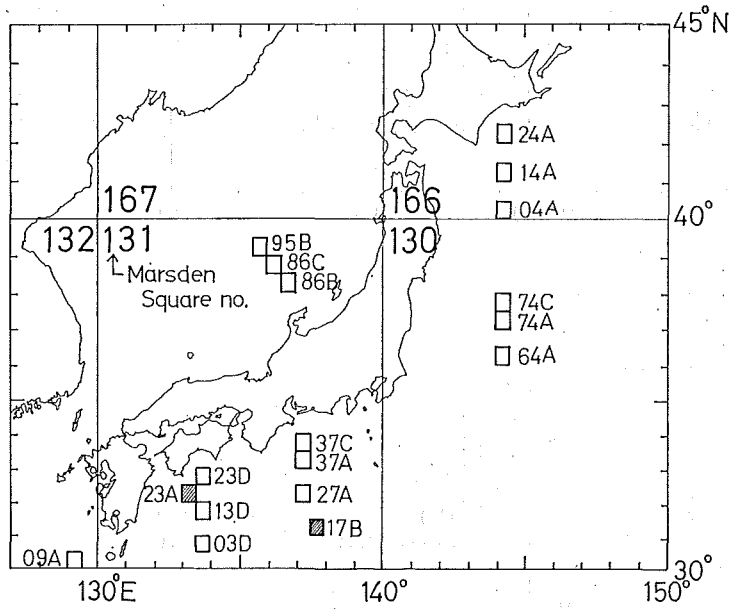

Figure 4 Selected 30′ meshes for which $\frac{1}{n}\sum_{i=1}^{n}(\Delta v_i)^2$, $V_{x\%}/V_{100\%}$ and relative frequency distribution of $\overline{V}$ are calculated

we get from (4)

$$\sigma^2=\overline{V}^2+\frac{1}{n}\sum_{i=1}^{n}(\Delta v_i)^2-\overline{V}^2 \ . \qquad (5)$$

Here we assume that

$$\frac{1}{n}\sum_{i=1}^{n}(\Delta v_i)^2=\alpha^2\sigma^2 \ , \qquad (6)$$

where α^2 is coefficient to be determined empirically.

If this assumption that the variance of the scalar is proportional to that of the

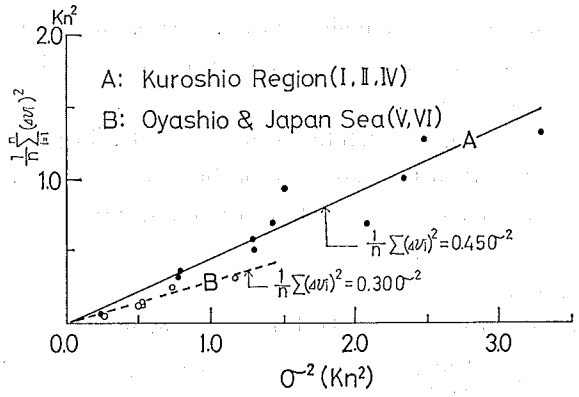

Figure 5 Pelationship between σ^2 and $\frac{1}{n}\sum_{i=1}^{n}(\Delta v_i)^2$ where $\Delta v_i=V_i-\overline{V}$

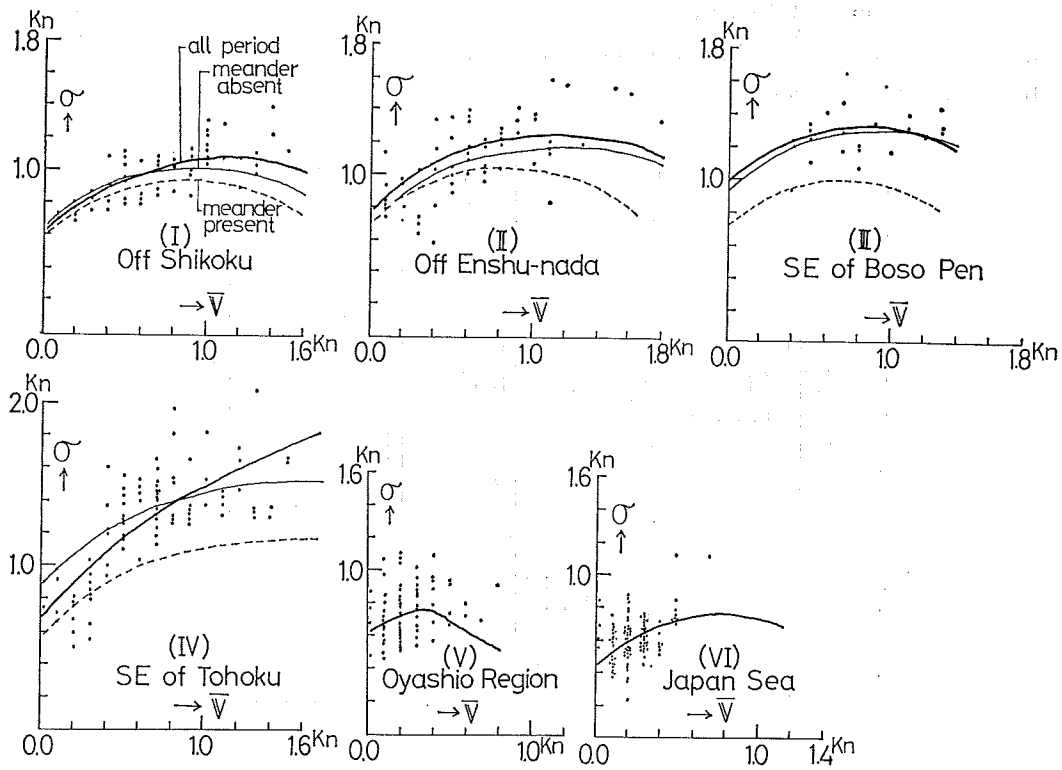

Figure 6 Relationship between σ and $\overline{V}$ with the statistical values im the Period A and the calculated lines for the Periods A, B and C

velocity is usable, we get

$$\sigma^2=\frac{1}{1-\alpha^2}(\overline{V}^2-\overline{\boldsymbol{V}}^2)\ . \tag{7}$$

Substituting (1) into (7),

$$\sigma^2=\frac{1}{1-\alpha^2}\{(a^2-1)\overline{\boldsymbol{V}}^2+2ab\overline{\boldsymbol{V}}+b^2\} \tag{8}$$

or

$$\sigma^2=\frac{1}{a^2(1-\alpha^2)}\{(a^2-1)\overline{V}^2+2b\overline{V}-b^2\} \tag{9}$$

is obtatined with regard to $\overline{\boldsymbol{V}}$ or $\overline{V}$ together with a and b.

To make sure of the availability of the assumption in (6), σ^2 and $\frac{1}{n}\sum_{i=1}^{n}(\Delta v_i)^2$ in eighteen meshes (Figure 4) for all the period selected from places on the axial areas of the Kuroshio, Oyashio and Tsushima Current and both sides of the Kuroshio axis in the Regions I and II are plotted in Figure 5. We get approximately linear relationship between σ^2 and $\frac{1}{n}\sum_{i=1}^{n}(\Delta v_i)^2$. The value of α^2 is 0.45 for the Kuroshio region (Regions I-IV) and 0.30 for the other regions.

Through the differentiation of (8) or (9) with $\overline{\boldsymbol{V}}$ or $\overline{V}$ respectively, we can easily find that σ becomes maximum when

$$\overline{\boldsymbol{V}}=\frac{ab}{1-a^2} \tag{10}$$

or

$$\overline{V}=\frac{b}{1-a^2}\ . \tag{11}$$

The relations between σ and $\overline{\boldsymbol{V}}$ are shown in Figure 6. The deviations of the statistical values from the curves calculated by (8) seem to be larger in some extent than the cases of $\overline{\boldsymbol{V}}\sim\overline{V}$ and $\overline{\boldsymbol{V}}\sim S$, especially for the range of large $\overline{\boldsymbol{V}}$ in the Regions V and VI. Small values of the regression coefficients between $\overline{\boldsymbol{V}}$ and $\overline{V}$ in the Oyashio region and the Japan Sea, which lead to rough estimation of a and b, may be one of the reasons.

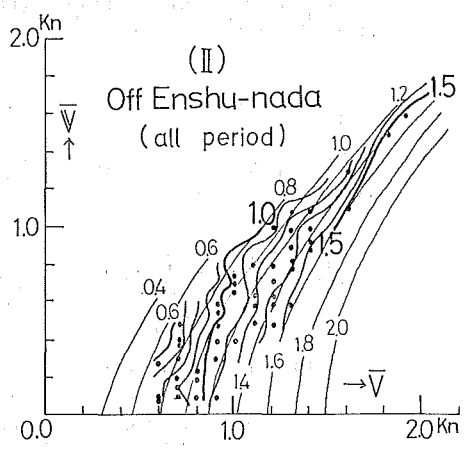

Figure 7 Value of σ as the function of $\overline{V}$ and $\overline{\boldsymbol{V}}$

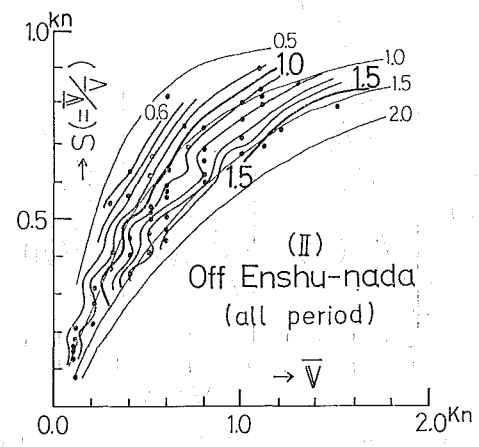

Figure 8 Value of σ as the function of $\overline{\boldsymbol{V}}$ and S

As seen from (7), σ may be also expressed by $\overline{V}$ and $\overline{V}$, and it increases with increasing $\overline{V}$ and decreases with increasing $\overline{V}$ (Figure 7).

Moreover, we get

$$\sigma=\frac{\overline{V}}{S}\sqrt{\frac{1-S^2}{1-\alpha^2}} \tag{12}$$

from (7) with the use of $\overline{V}$ and S. It is seen from Figure 8 that σ increases with increasing $\overline{V}$ and decreasing S as can be expected by the simple consideration.

The value of σ decreases with increasing $\overline{V}$ in Figure 7, but it increases with increasing $\overline{V}$ in Figure 8. This may be seemed to contradict to each other, but this apparent contradiction is due to the fact that σ is regarded as the function of $\overline{V}$ and $\overline{V}$ or $\overline{V}$ and S, where $\overline{V}$ and S are the functions of $\overline{V}$ as show in (1) and (2). According to (2), (3), (8) and (9), S and σ are expressed by a, b and $\overline{V}$ or a, b and $\overline{V}$, or in other words by $\overline{V}$ and $\overline{V}$ basically, where a and b regulate the relationship between $\overline{V}$ and $\overline{V}$ in each region.

(4) $V_{max}\sim\overline{V}$

The ratio $V_{max}/\overline{V}$ is about three on the average in each region as shown in Figure 9. However, so far as there is large difference in number of data used in each mesh,

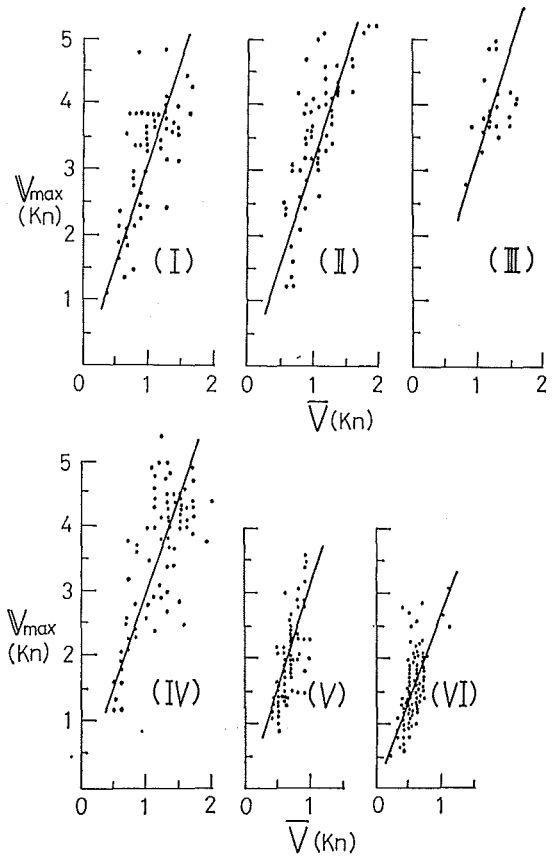

Figure 9 Relationship between V_{max} and $\overline{V}$

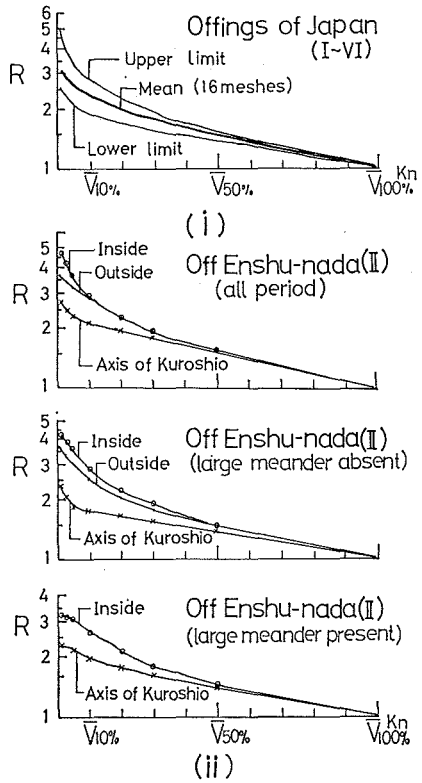

Figure 10 (i) : Mean, upper and lower limits of $\overline{V}_{x\%}/\overline{V}_{100\%}$
(ii) : $\overline{V}_{x\%}/\overline{V}_{100\%}$ on the mean axial area, inside and outside of the Kuroshio off Enshu-nada

it is better to use the average of the highest values of the certain percentages instead of V_{max} as a statistical measure of the highest speed, though the vector sense will be ignored.

Figure 10 (i) shows the mean, upper and lower limits of $\overline{V}_{x\%}/\overline{V}_{100\%}$ by the use of data in the sixteen selected meshes arround the Japan shown by white squares in Figure 4, where the scalar mean of the highest $x\%$ of the total number of the data in each mesh is written with $\overline{V}_{x\%}$. The ratios $\overline{V}_{1\%}/\overline{V}_{100\%}$ in all meshes fall in the range of 2.5–5 and their mean is about 3.0 nearly coinciding with Figure 9.

As shown in Figure 10 (ii), the ratios $\overline{V}_{x\%}/\overline{V}_{100\%}$ on the mean axial area of the Kuroshio off Enshu-nada in every statistical periods are less than those in the both sides of it owing to the large effect of the shifting of the current axis to north and south from time to time on the increases of ratios $\overline{V}_{x\%}/\overline{V}_{100\%}$ in the both sides of the axial area, especially for the range of small value of x.

6. Relative Frequency Distribution

The relative frequency distributions in the eighteen 30′ meshes shown in Figure 4 with square have been computed with every interval of 0.4 knots of the speed (Figure 11).

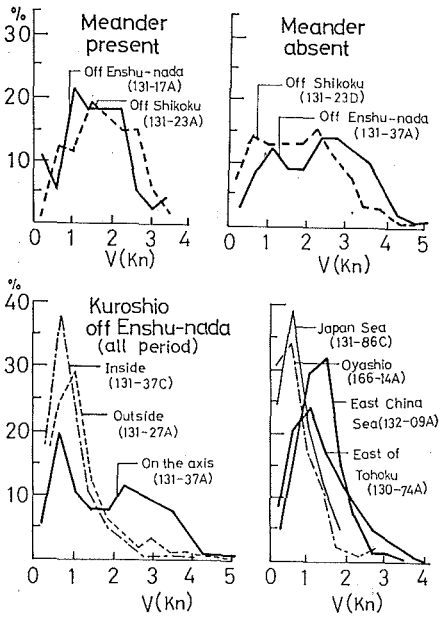

Figure 11 Relative frequency distributions of the speed in the Kuroshio region (Off Shikoku, Enshu-nada, in the East China Sea and Kuroshio extension), the Oyashio region and the Japan Sea

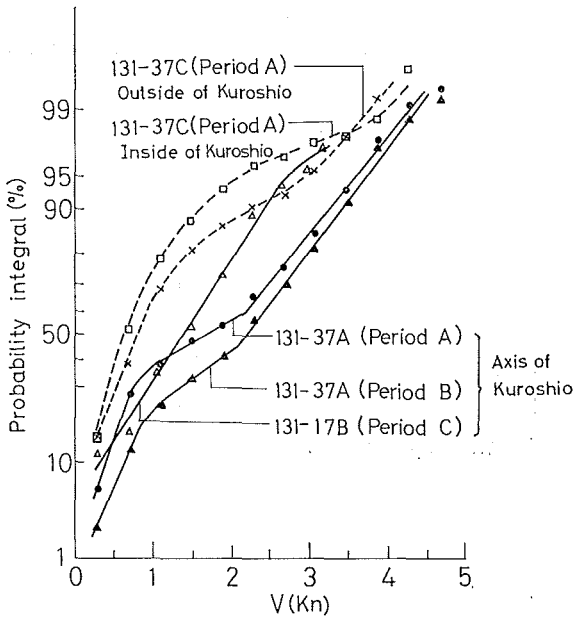

Figure 12 Test by the normal distribution paper

The distribution curves in the Kuroshio axial area off Shikoku and Enshu-nada show the different modes in each statistical period. In the Period C, in which the large meander of the Kuroshio exists, the distribution curve shows rough normal distribution

in general, though that in the range of high velocities does not always coincide with it. On the other hand, the curve has two peaks, especially off Enshu-nada, corresponding to low and high speed ranges (about 0.7–1.1 and 2.3–2.7 knots) in the Period B. These modes are shown in Figure 12 with the use of normal probability paper.

In the Period A, the curve for axial area of the Kuroshio off Enshu-nada also has two peaks. All curves for the places of inside and outside of the Kuroshio are biased to the lower speed side. These distributions are nearly logarithmic normal distribution according to the tests by the logarithmic normal probability paper.

The curves for the Kuroshio axial areas in the East China Sea and the Kuroshio extension as well as the Oyashio region and the Japan Sea are also nearly logarithmic normal distribution. This coincides with the report of Paquette (1972). He indicates that the probability distribution of the currents observed by moored current meters are nearly logarithmic normal distribution (i.e. 34 out of 43 cases to 5% significance or better).

7. Seasonal Variation

The seasonal variation of each statistical element in the Kuroshio region (Regions I–IV) is not neglegible. It has been already pointed out that the velocity of the Kuroshio axial area has the seasonal variation (Masuzawa, 1960 and 1965; Taft, 1972; Nitani, 1969 and 1975).

As shown in Figure 13, the annual variation of each statistical element is clear.

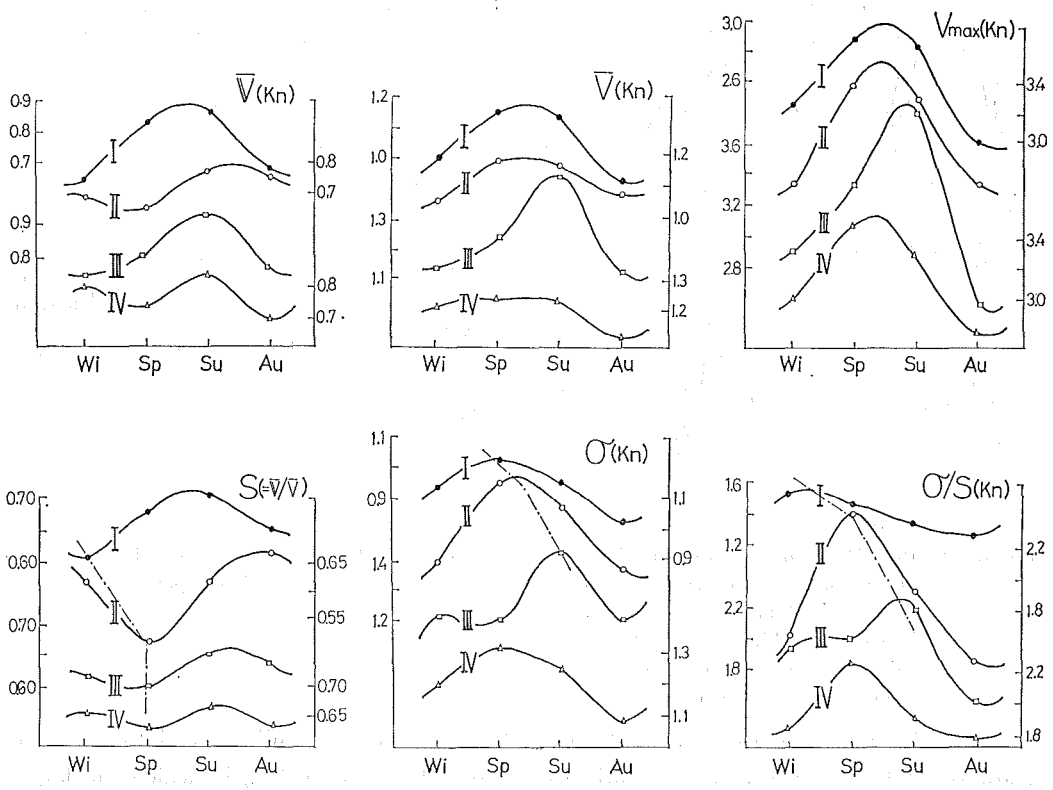

Figure 13 Seasonal variations of $\overline{V}$, $\overline{V}$, V_{max}, S, σ and σ/S

$\overline{V}$ and V_{max} have similar pattern except in the Region IV, and their maxima appear in early and mid summer and minima in mid and late autumn. The pattern of $\overline{V}$ is a little different from those of $\overline{V}$ and V_{max}. These patterns, however, progress from the Region I to the Region III (west-east) spending 1–2 months in accordance with the results of Taft and Nitani.

The minimum of the stability and the maximum of the standard deviation start the Region I in winter and spring and reach to the Region III in spring and summer, respectively. The maximum of the product of standard deviation and the reciprocal of stability, σ/S, which can be considered as a comprehensive measure of the variability of the velocity and we call it the variability tentatively hereafter, starts the Region I in late winter and reaches to the Region III in early summer with a mean phase velocity of about 3.5 nauti. mile/day. This value is less than the value of 4.8 nauti. mile/day, which is the mean easterly phase velocity of the small- and medium-scale meanders between the offings of Shikoku and Enshu-nada (Nitani, 1975). Taking account of the facts that they may take much time to across the Izu Ridge and that the statistical period in Figure 13 includes the Period C (large meander present), in which large meander has phase velocity of nearly zero and the appearance of the small- and medium-scale meanders is very rare, the averaged phase velocity between the Region I and the Region III mentioned above may be appropriate substantially. We can not find the farther progression of the variability of the Kuroshio from the Region III to the Region IV where another motive force relating to the Oyashio region might act in certain manner.

8. Concluding Remarks

Although each element has own characteristic distributional pattern in each region, but the pattern of each element is similar to each other within the same region, especially in the Kuroshio region.

According to the consideration in Section 5, $\overline{V}$ is linear funcsion of $\overline{V}$, and other two elements, S and σ, are the comparatively simple functions of $\overline{V}$ and $\overline{V}$ or $\overline{V}$ and the constants a and b which have the specific values in the individual region shown in

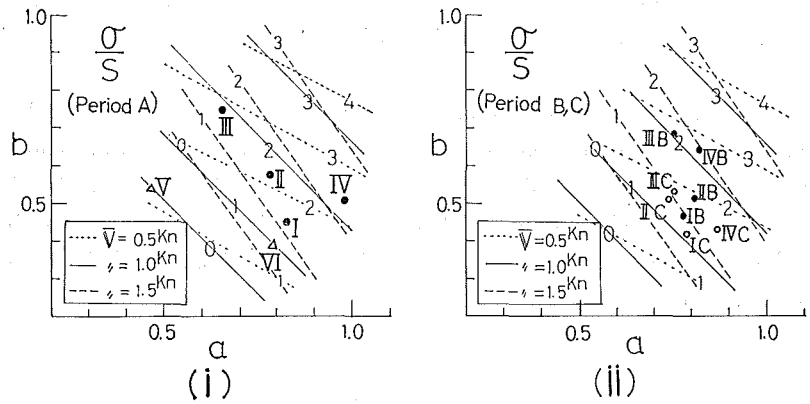

Figure 14 Relationship between a and b in each region and the value of σ/S as the function of a, b and $\overline{V}$ for the Period A in (i) and the Periods B and C in (ii)

Figure 1 and regulate the linear relation between $\overline{V}$ and $\overline{V}$ in that region. This may be the main reason for the similar distributional pattern of each element in individual region, especially in the Kuroshio region. Thus, the characteristical constants a and b in (1), together with $\overline{V}$, are the basic quantities for the various characteristics of the current in each region including the variational characteristic of the current.

The relation between a and b of each region is shown in Figure 14 together with the value of the variability σ/S. The rough linear relation is found in the Kuroshio region in each period, though the reason for its mechanism is unknown.

The values $\overline{V}$, S and σ are the functions of $\overline{V}$ and $(a\overline{V}+b)$. Also σ/S is expressed by

$$\frac{\sigma}{S}=\left[\frac{1}{1-\alpha^2}\left\{\frac{(a\overline{V}+b)^4}{\overline{V}^2}-(a\overline{V}+b)^2\right\}\right]^{1/2}, \tag{13}$$

as the function of $\overline{V}$ and $(a\overline{V}+b)$ together with α^2. According to Figure 14, the variability σ/S becomes larger with increasing a and b, and in general, it decreases with increasing $\overline{V}$ for not so large a.

In the Kuroshio region (Regions I–IV) except Region IV for the case in which $\overline{V}$ is 0.5 knots (in Figure 14), the variability becomes larger with the distance from the Region I in every statistical periods. Moreover, in each region the variability in the Period B is larger than that in the Period C, especially for the Region III and IV. Accordingly, Figure 14 may be one proof for the facts that the small- and medium-scale meanders of the Kuroshio progress to east increasing their scale with the distance in the Period B, that these meanders occur less frequently in the Period C than in the Period B and that even if they occur they hardly reach to the Region III across the Izu Ridge in the Period C.

Further statistics such as those on the long-term variation of each element will be conducted in the future. Also, preparation of atlases with use of the statistical results for every 15′ meshes in latitude and longitude after more accumulation of GEK data may be useful. For the analysis of the statistical results, the reconsideration in selecting or subdividing of the representative regions not only for the Kuroshio region but also for the other regions such as the Japan Sea and the Oyashio region may be necessary for our more appropriate understandings of the currents from the view-point of the statistics.

The authors are indebted to all members of Japan Oceanographic Data Center (JODC) for carrying out of this current statistics and preparation of the manuscript. To Dr. Akira M. Shinzi, Hydrographic Department, we are also indebted for his critical reading of the manuscript. The authors wish to express their hearty thanks to all Japanese scientists who have engaged in the oceanographic investigations for their efforts to accumulate the vast current data.

Reference

Hydrographic Office, US Navy 1964: *Atlas of surface currents, Northwestern Pacific Ocean*, H.O. Pub. No. 569, 1–12.

Hydrographic Office, Japanese Navy 1935: *Atlas of the currents in the seas adjacent to Japan,* Secret Pub. No. 555-1048, 1-22. (in Japanese)

Hydrographic Office, Japanese Navy 1936: *Atlas of the currents in the North Pacific Ocean,* No. 6031, 1-4. (in Japanese)

Masuzawa, J. 1960: Statistical characteristics of the Kuroshio current, *Oceanogr. Mag.,* **12,** 7-15.

Masuzawa, J. 1965: A note on the seasonal variation of the Kuroshio velocity, *J. Oceanogr. Soc. Japan,* **21,** 117-118. (in Japanese)

Nitani, H. 1969: On the variability of the Kuroshio in recent several years, *Bull. Japan Soc. Fish. Oceanogr.,* **14,** 13-18. (in Japanese)

Nitani, H. 1974: Effect of the Kuroshio system on the sea level at the southern coast of Japan, *Rep. Hydrogr. Res.,* No. 9, 51-70.

Nitani, H. 1975: Variation of the Kuroshio south of Japan, *J. Oceanogr. Soc. Japan,* **31,** 154-173.

Paquette, R. 1972: Some statistical properties of ocean currents, *Ocean Eng.,* **2,** 95-114.

Rikiishi, K. 1974: Note on the Kuroshio meander, *J. Oceanogr. Soc. Japan,* **30,** 42-45.

Rikiishi, K., Umatani, S. 1977: Characteristic features of the Kuroshio with and without the cold water mass south of Enshunada, *Rep. Res. Inst. Appl. Mech.,* **XXV,** No. 79, 79-101.

Taft, B. 1972: Characteristcs of the flow of the Kuroshio south of Japan, *Kuroshio-Its physical aspects,* Ed. H. Stommel and K. Yoshida, Univ. Tokyo Press, 165-216.

US Naval Oceanographic Office 1964: *Ocean currents in the vicinity of the Japanese Islands and China Coast,* 2nd edition, Pub. No. 237, 1-14.

US Naval Oceanographic Office 1977: *Surface currents, North Pacific Ocean and Sea of Japan,* NOO SP 1402, 1-18.

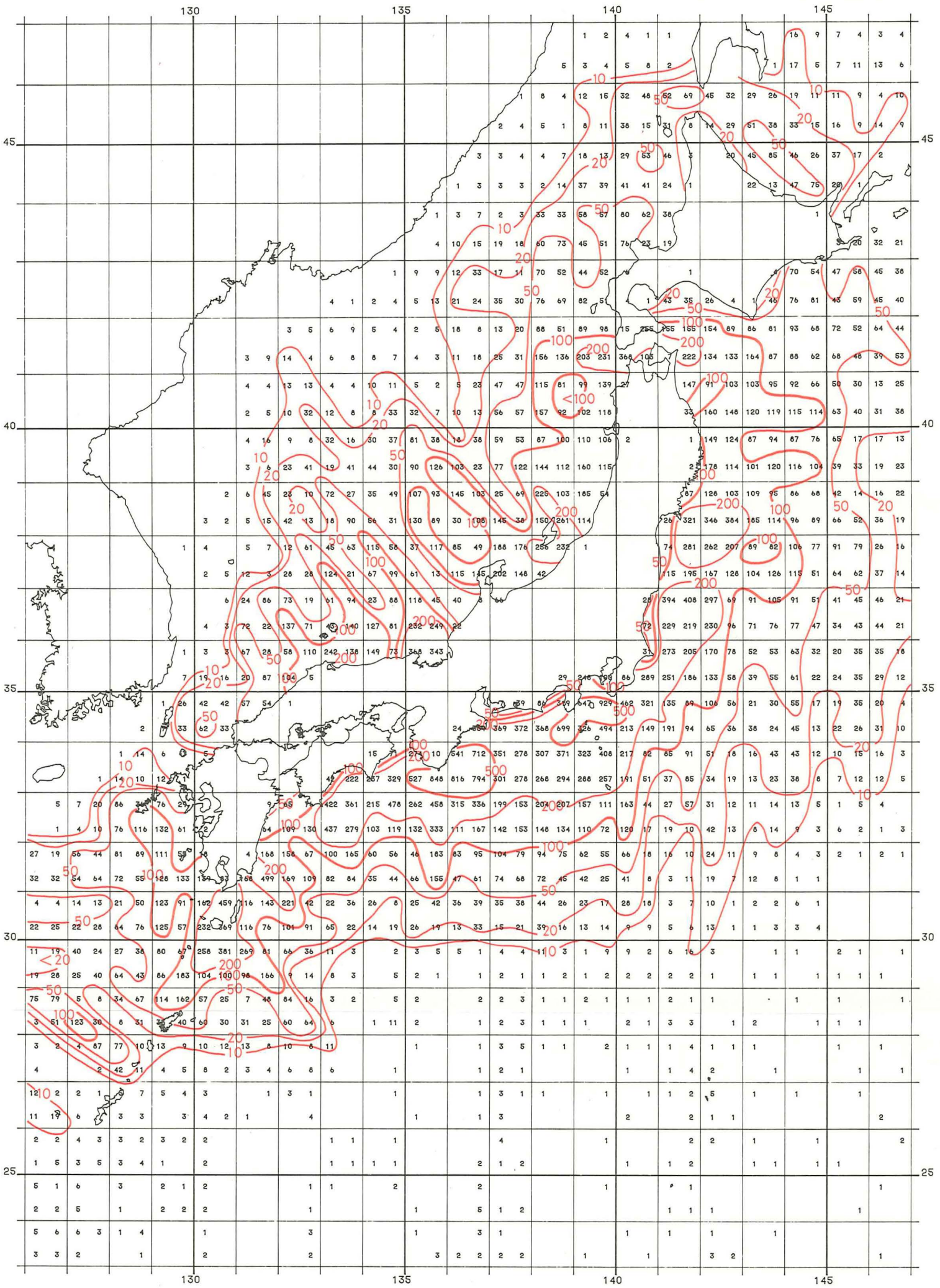

Plate 1 Number of the data used in the statistics for all the period (Period A)

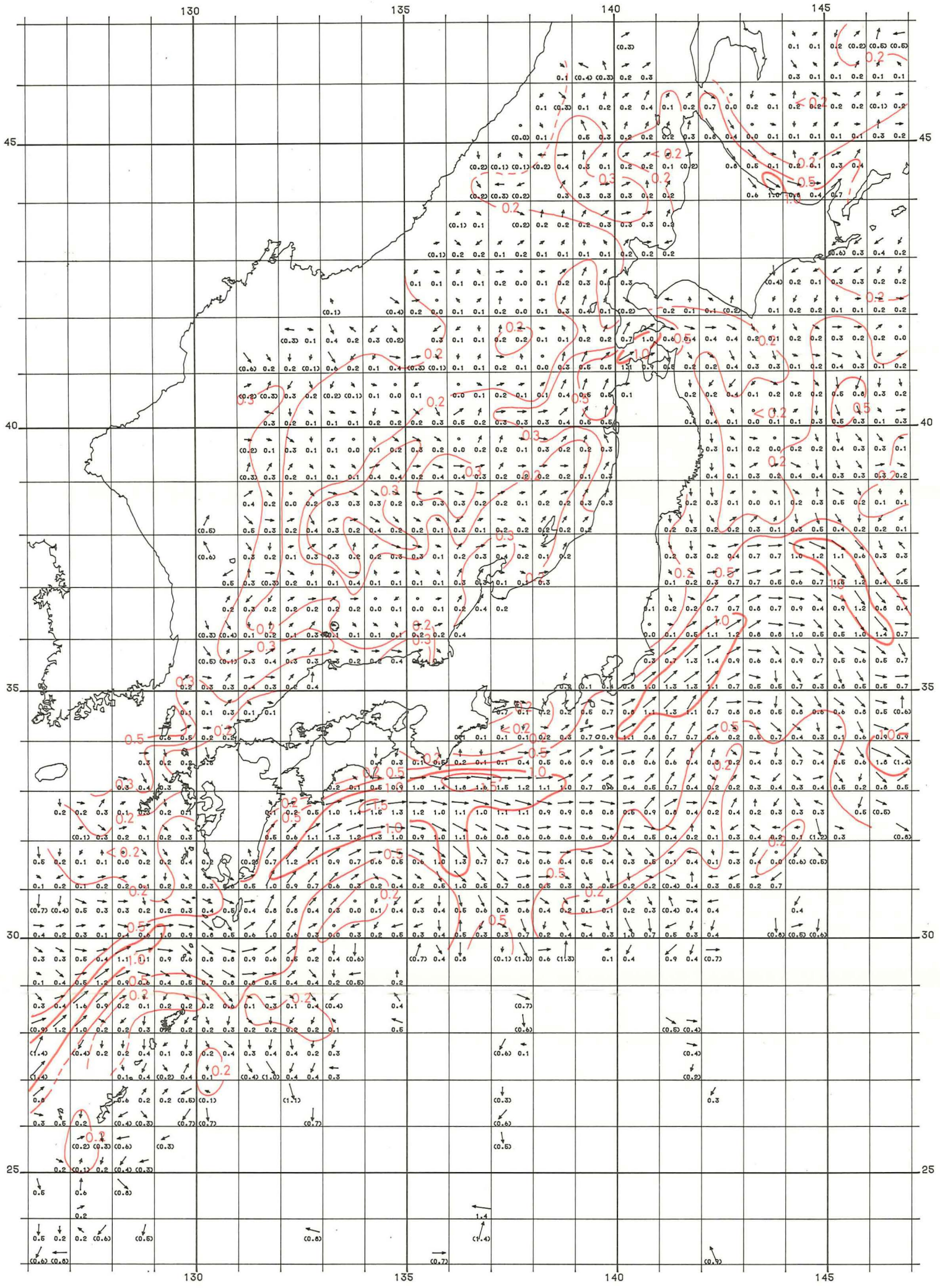

Plate 2 Vector mean $\overline{V}$ for all the period (Period A) in knots

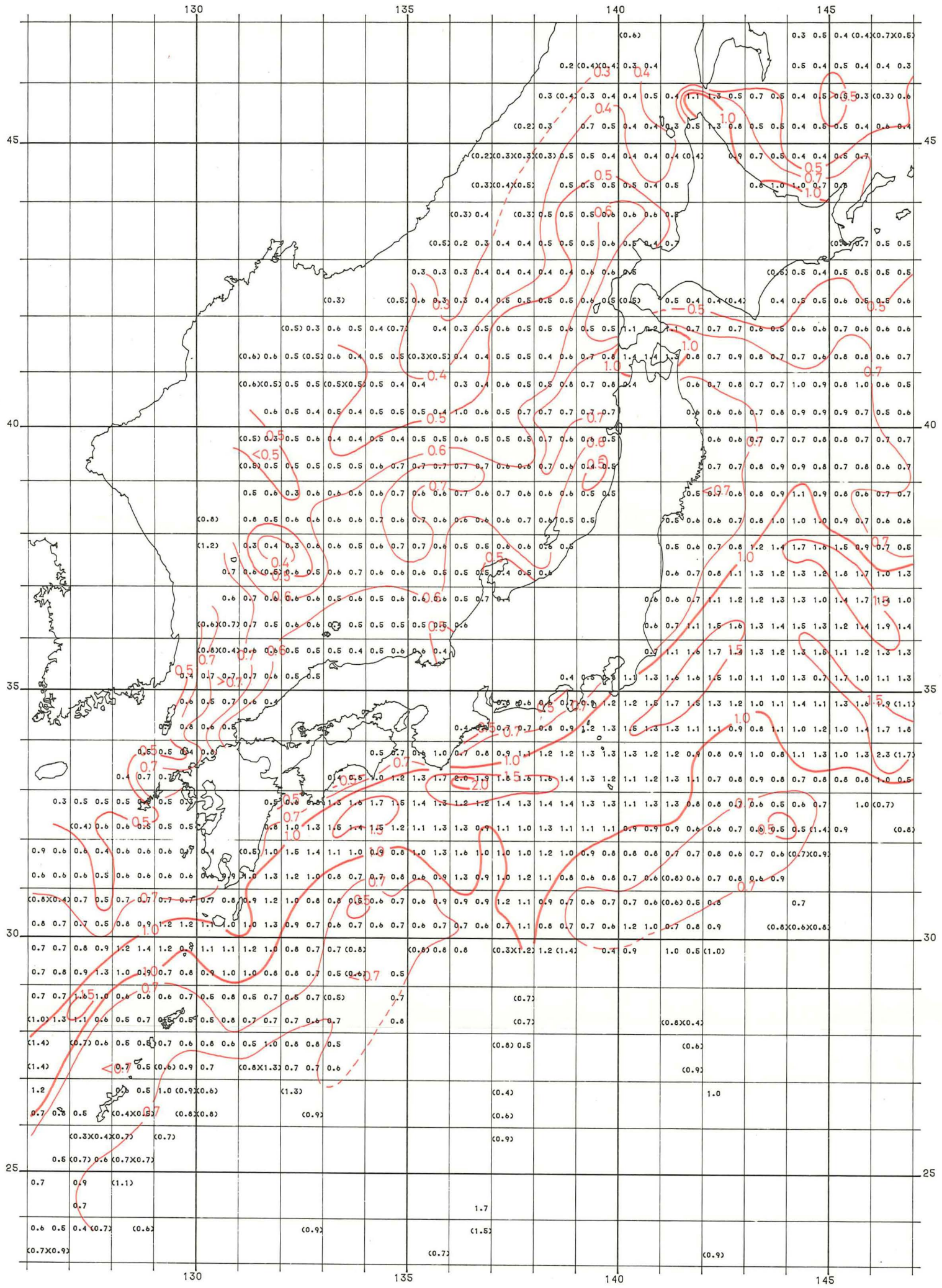

Plate 3 Scalar mean $\overline{V}$ for all the period (Period A) in knots

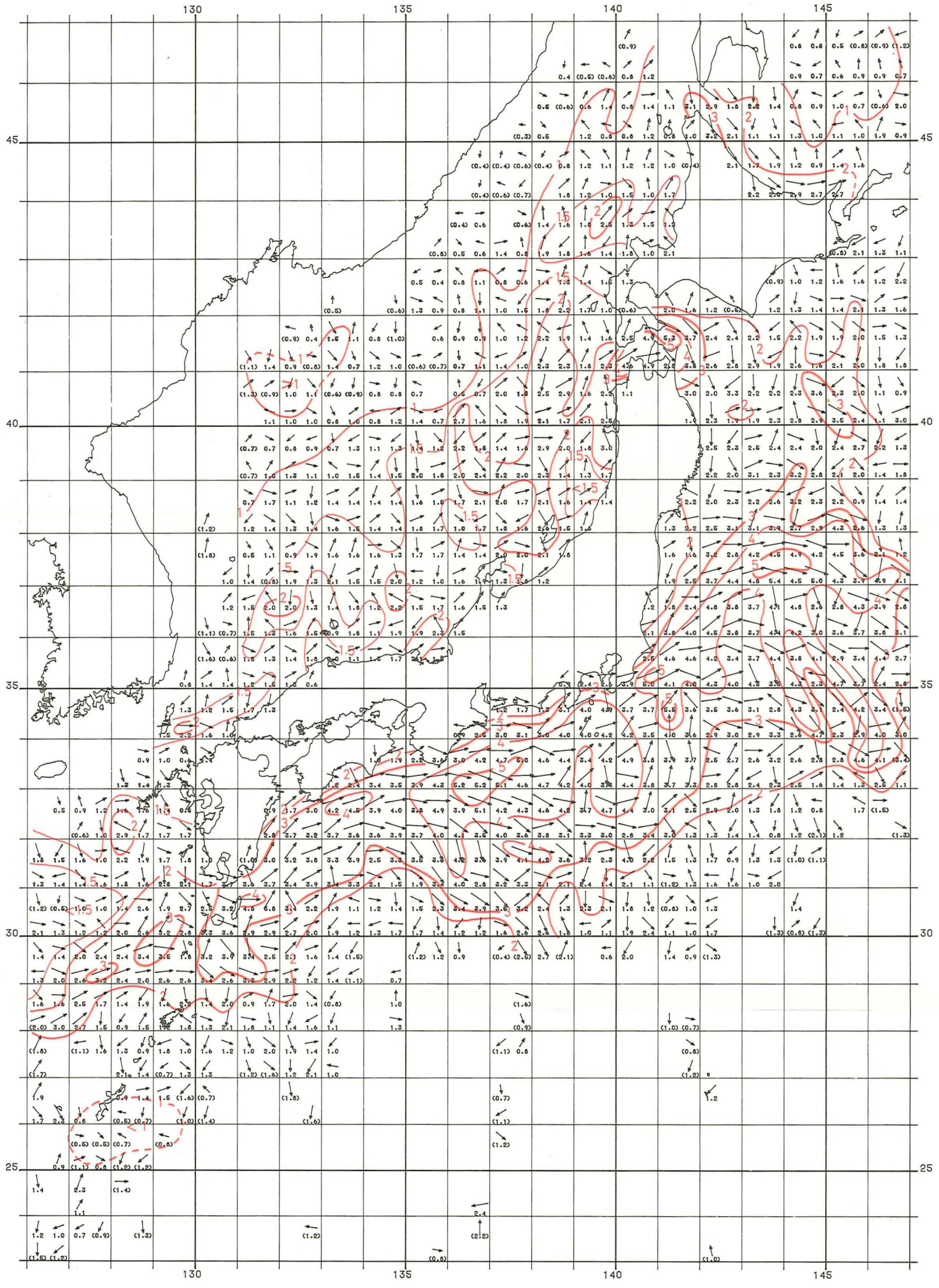

Plate 4 Maximum velocity V_{max} for all the period (Period A)

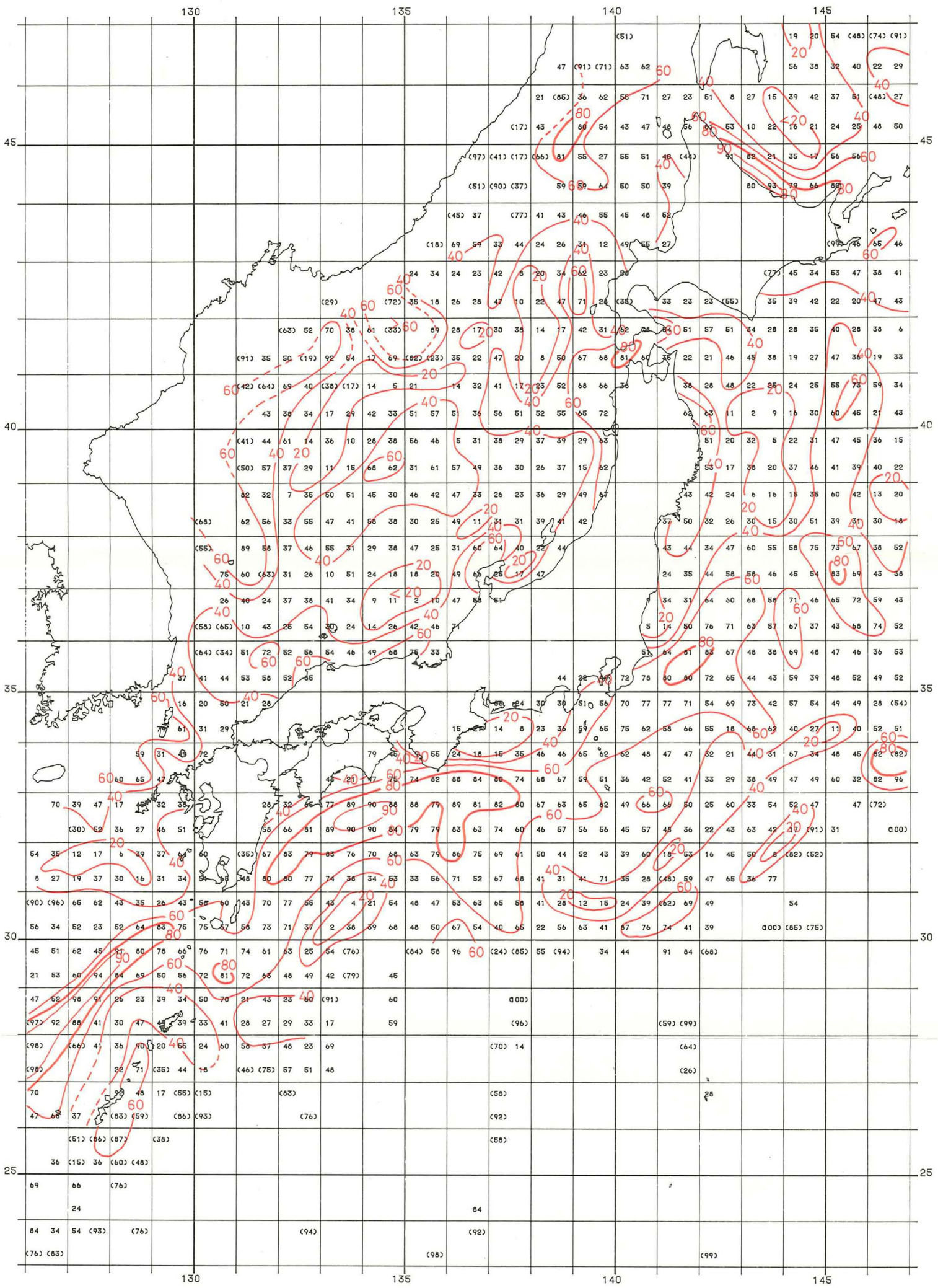

Plate 5 Stability S $(=\overline{V}/\overline{V})$ for all the period (Period A) in %

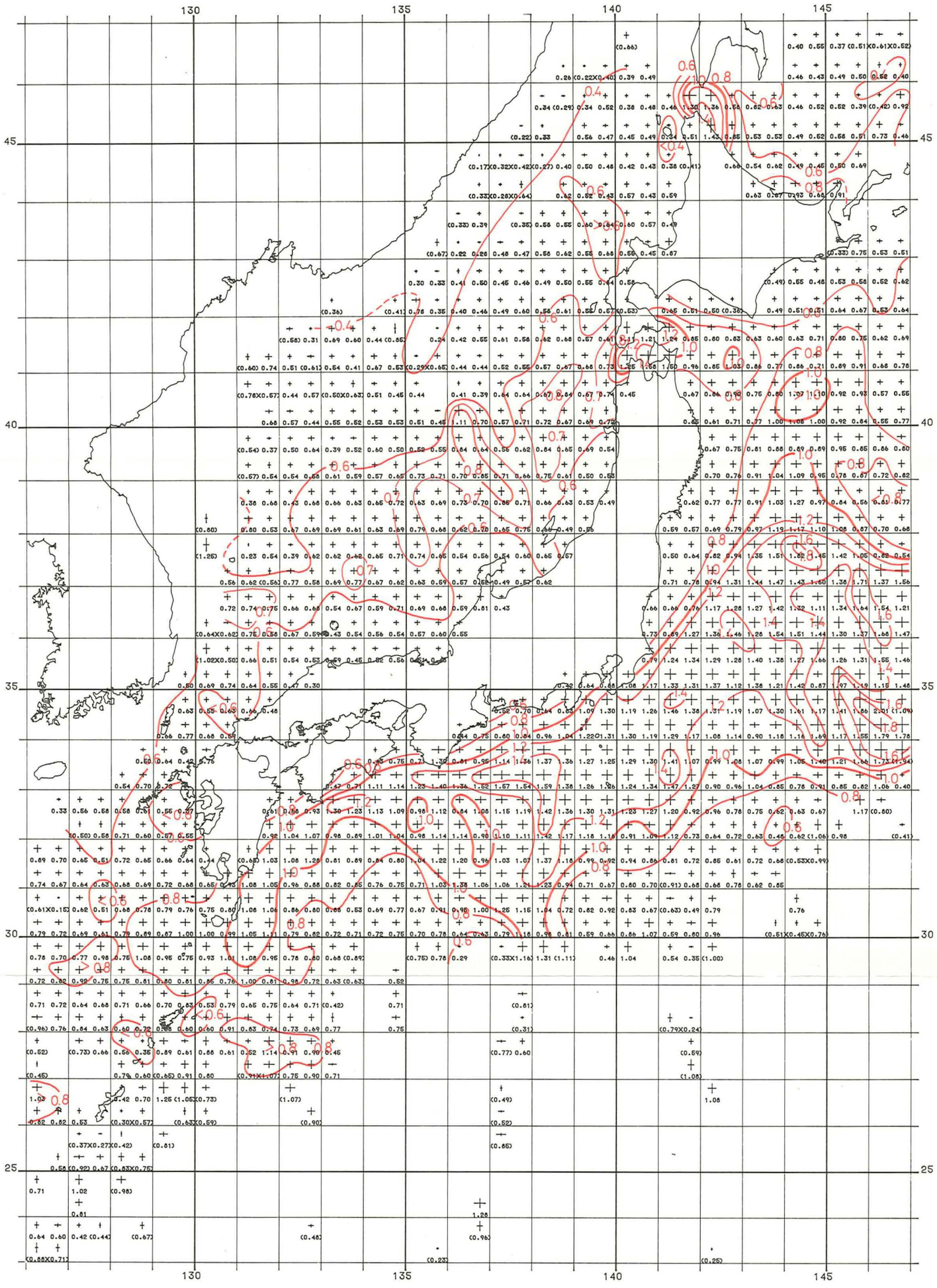

Plate 6 Standard deviation σ for all the period (Period A) in knots

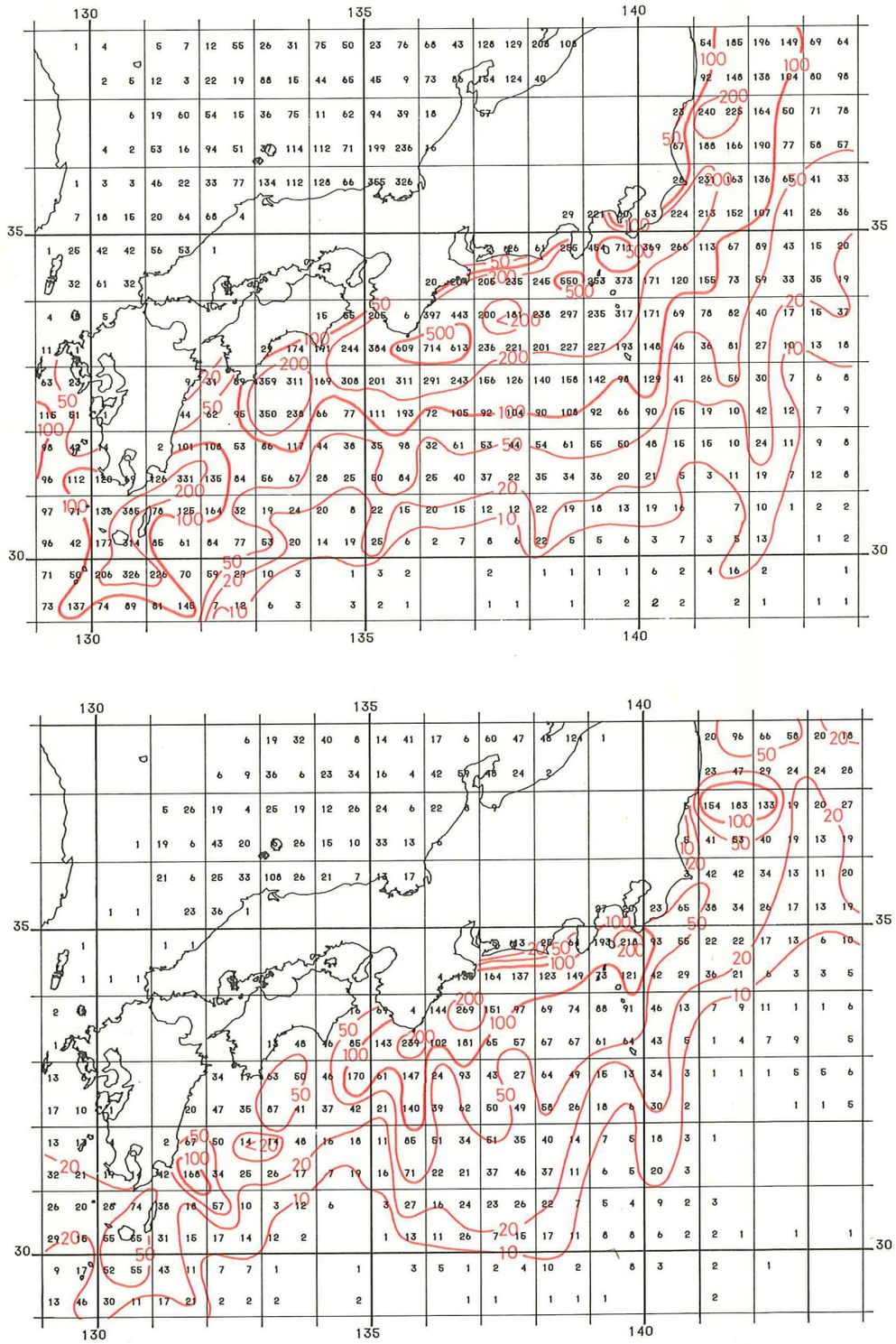

Plate 7 Number of the data used in the statistics for the Periods B (upper) and C (lower)

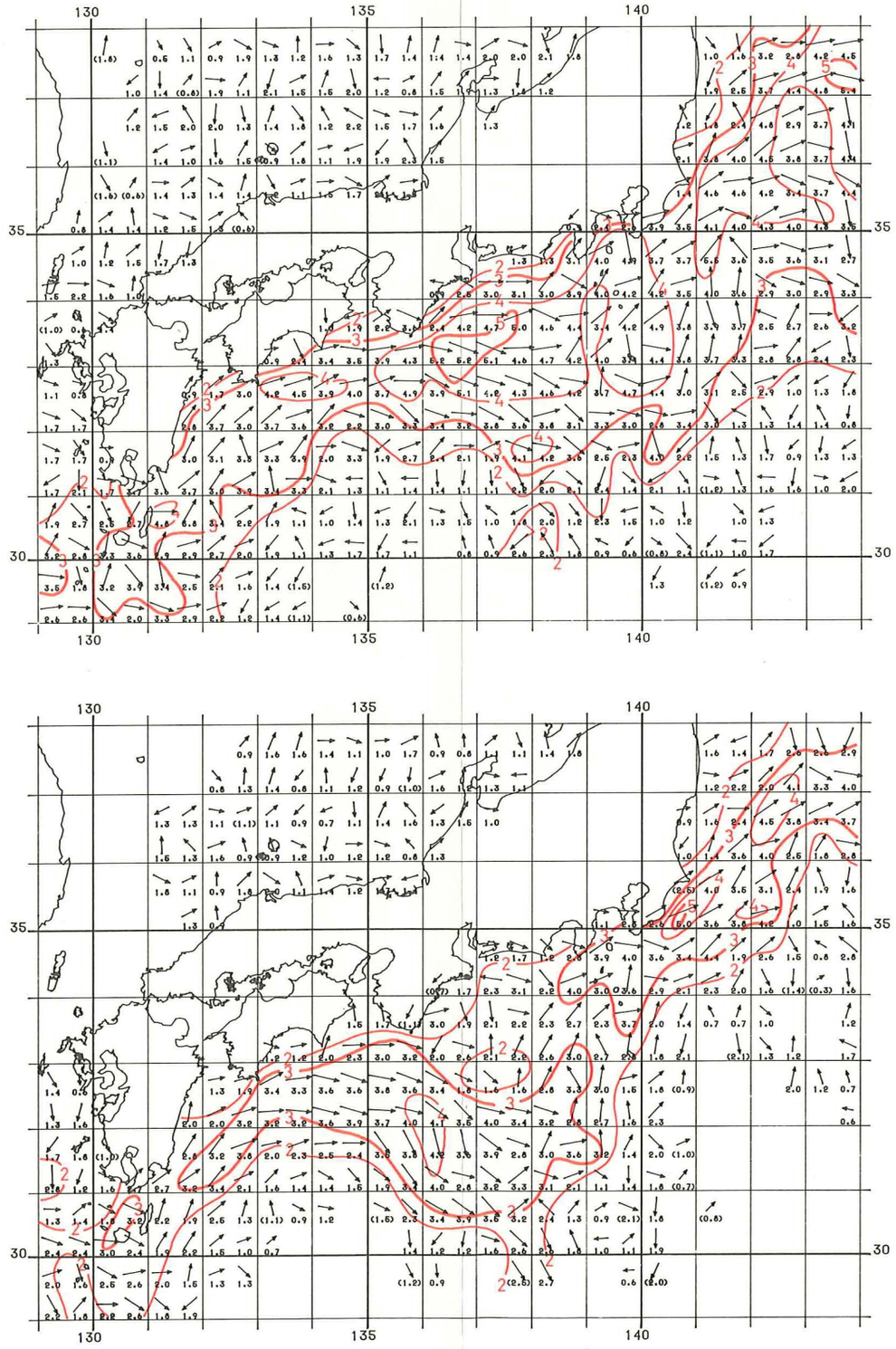

Plate 8 Maximum velocity *Vmax* for the Periods B (upper) and C (lower) in knots

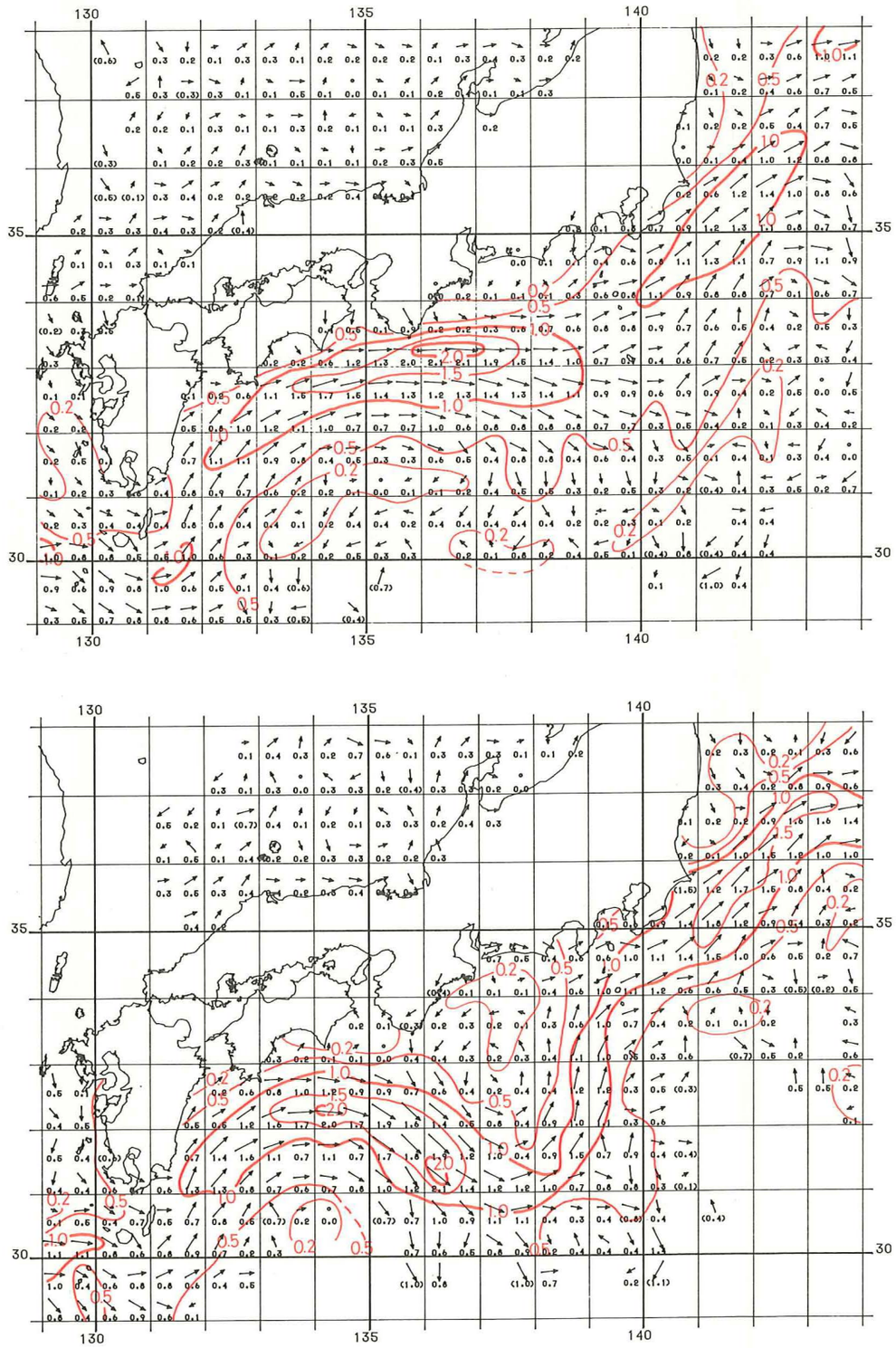

Plate 9 Vector mean $\overline{V}$ for the Periods B (upper) and C (lower) in knots

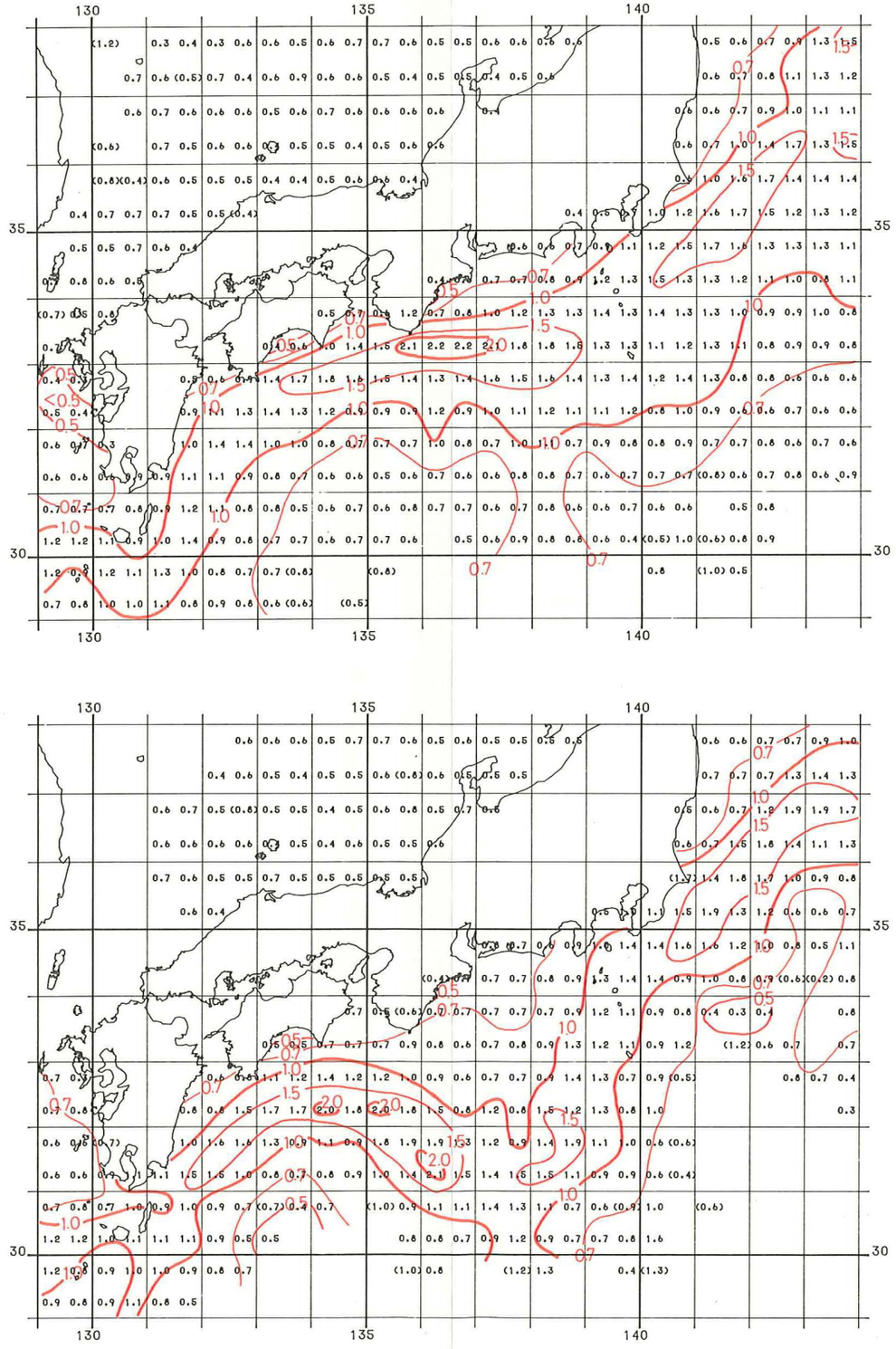

Plate 10 Scalar mean $\overline{V}$ for the Periods B (upper) and C (lower) in knots

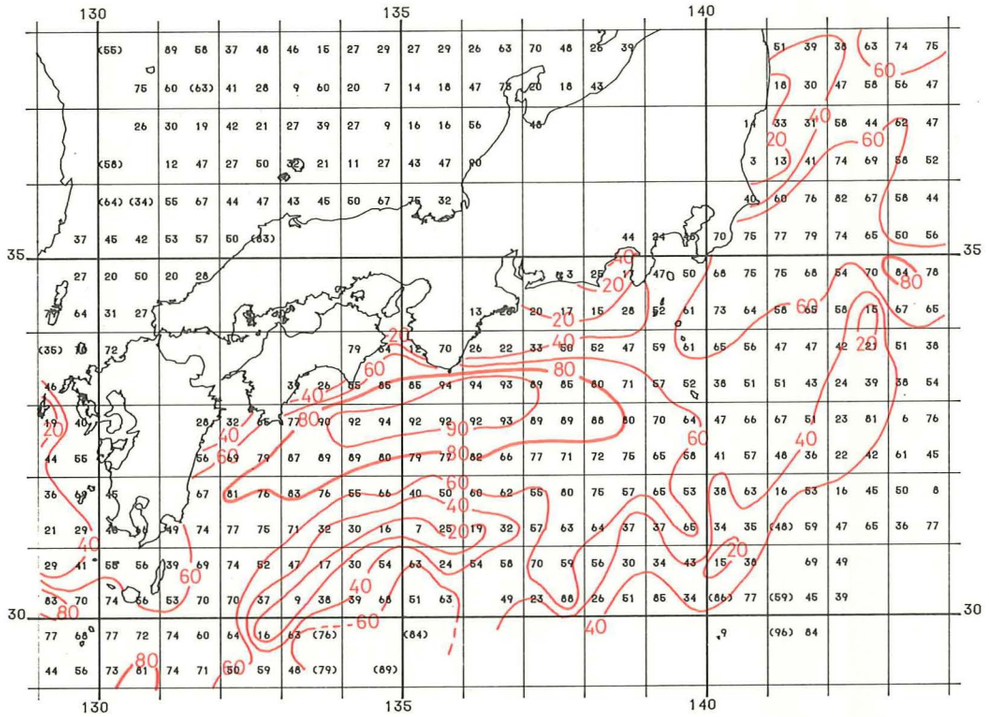

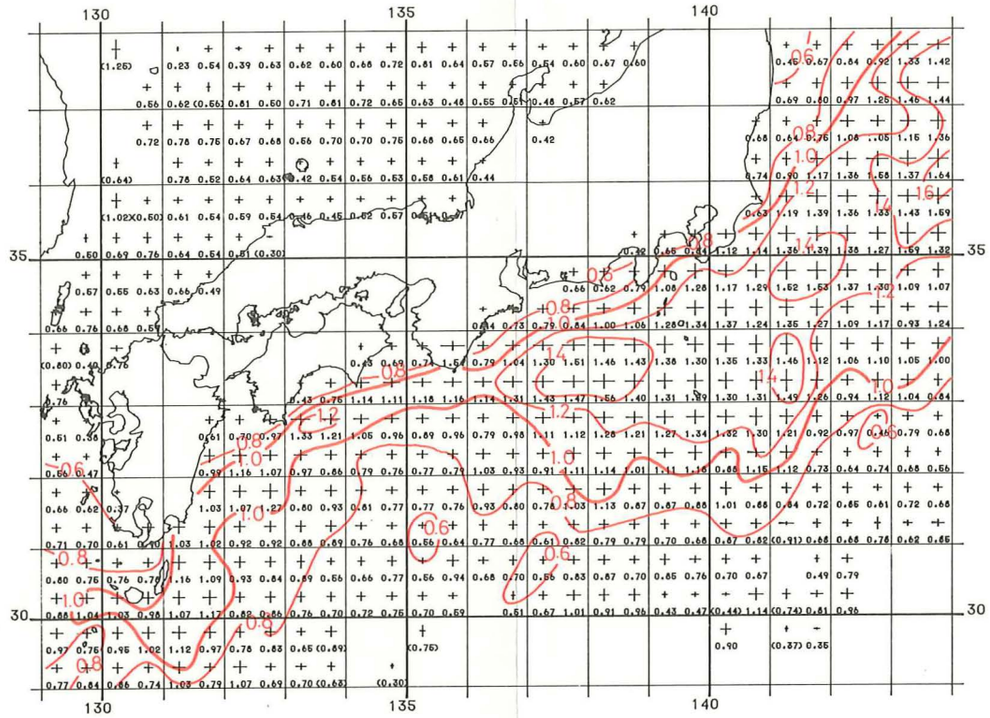

Plate 11 Stability S $(=\overline{V}/\overline{V})$ for the Periods B (upper) and C (lower) in %

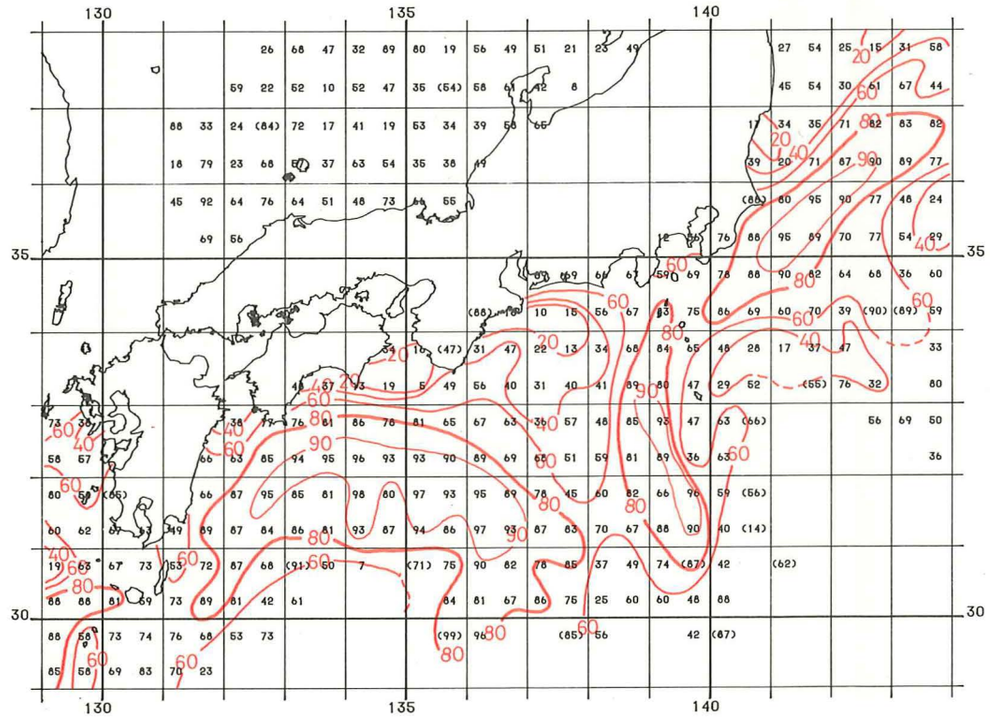

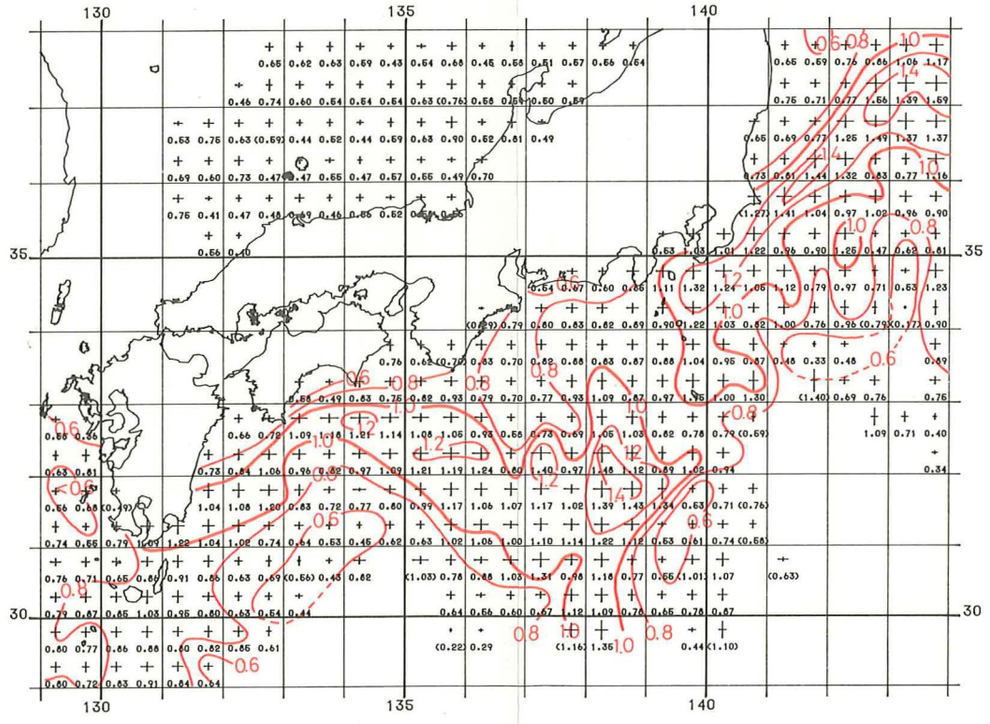

Plate 12 Standard deviation σ for the Periods B (upper) and C (lower) in knots